

PAPER • OPEN ACCESS

## High pressure torsion induced structural transformations in Ti- and Zr-based amorphous alloys

To cite this article: D V Gunderov *et al* 2018 *IOP Conf. Ser.: Mater. Sci. Eng.* **447** 012052

View the [article online](#) for updates and enhancements.



**IOP | ebooks™**

Bringing you innovative digital publishing with leading voices to create your essential collection of books in STEM research.

Start exploring the collection - download the first chapter of every title for free.

# High pressure torsion induced structural transformations in Ti- and Zr-based amorphous alloys

D V Gunderov<sup>1,3</sup>, E V Boltynjuk<sup>2</sup>, E V Ubyivovk<sup>2</sup>, A A Churakova<sup>1,3</sup>,  
G E Abrosimova<sup>4</sup>, V D Sitdikov<sup>1</sup>, A R Kilmametov<sup>5</sup>, R Z Valiev<sup>1,2</sup>

<sup>1</sup>Ufa State Aviation Technical University, 12 K. Marx str., Ufa 450008, Russia

<sup>2</sup> Saint Petersburg State University, 28 Universitetskiy pr., Saint Petersburg 198504, Russia

<sup>3</sup>Institute of Molecule and Crystal Physics - Subdivision of the Ufa Federal Research Centre of the Russian Academy of Sciences, Prospekt Oktyabrya 151, Ufa, 450075, Russia

<sup>4</sup> Institute of Solid State Physics Russian Academy of Sciences, 2 Academician Ossipyan str., Chernogolovka, Moscow District, 142432, Russia

<sup>5</sup>Karlsruhe Institute of Technology (KIT), Institute of Nanotechnology, Hermann-von-Helmholtz-Platz 1, 76344 Eggenstein-Leopoldshafen, Germany

E-mail: dimagun@mail.ru

**Abstract.** The melt-spun (MS) Ti<sub>50</sub>Ni<sub>25</sub>Cu<sub>25</sub> alloy and the Zr<sub>62</sub>Cu<sub>22</sub>Al<sub>10</sub>Fe<sub>5</sub>Dy<sub>1</sub> bulk metallic glass (BMG) were subjected to high pressure torsion (HPT). X-ray diffraction (XRD) measurements show a shift of the first diffraction halo to a low angle after HPT processing, which corresponds to an increase in the values of the radius of the first coordination sphere and the free volume. Direct density measurements confirmed an increase in free volume values. A special TEM procedure was used for a detailed study of the microstructure of both amorphous alloys after HPT processing. The study revealed the formation of a large density of shear bands (SBs) in both alloys. Nanocrystals are formed directly in shear bands as a result of strain-induced nanocrystallization. Amorphous nanoclusters with a size of 20 nm are formed in an amorphous matrix surrounding the SBs in the HPT-processed MS alloy Ti<sub>50</sub>Ni<sub>25</sub>Cu<sub>25</sub>. The formation of nanoclusters was not observed in BMG Zr<sub>62</sub>Cu<sub>22</sub>Al<sub>10</sub>Fe<sub>5</sub>Dy<sub>1</sub> after HPT processing.

## 1. Introduction

High pressure torsion (HPT) seems to be a promising method to form a high density of localized shear bands for structural transformations of amorphous alloys [1-6]. Plastic deformation also leads to changes in the mechanical properties of amorphous alloys [1-10]. However, the features of structural transformations occurring in amorphous alloys during HPT processing are not clear. Preparing lamellae for TEM from the cross section of the HPT-processed specimen using a focused ion beam (FIB) provides a new opportunity to study the structural features of amorphous materials processed by HPT. Important information about the structure of amorphous alloys is given by the free volume, which can be estimated



by the XRD method [1, 7]. A new unique method [11] provides the ability to measure the density of HPT-processed samples with small sizes and complex shapes.

In this work, the melt-spun (MS) Ti<sub>50</sub>Ni<sub>25</sub>Cu<sub>25</sub> alloy and the bulk metallic glass (BMG) Zr<sub>62</sub>Cu<sub>22</sub>Al<sub>10</sub>Fe<sub>5</sub>Dy<sub>1</sub> were subjected to HPT processing. Complex structural studies using TEM, XRD and density measurements were utilized to study the effect of HPT on the structure and properties of amorphous alloys of different chemical compositions.

## 2. Experimental

The Ti<sub>50</sub>Ni<sub>25</sub>Cu<sub>25</sub> ribbons with a thickness of 0.04 mm and a width of 2 mm were produced by the melt spinning technique. Cylindrical rods with a diameter of 5 mm and a length of 50 mm from the Zr<sub>62</sub>Cu<sub>22</sub>Al<sub>10</sub>Fe<sub>5</sub>Dy<sub>1</sub> BMG (Zr<sub>62</sub> BMG) were made by copper mould casting. Fragments of the ribbons and BMG were subjected to HPT under an applied pressure of 6 GPa at room temperature for 10 and 5 revolutions, respectively. The structure of the HPT-processed specimens was examined by TEM on a Zeiss Libra 200FE. Data on selected area electron diffraction (SAED) were collected from an area of 80 nm in diameter. To prepare the TEM samples from the cross section of the HPT-processed specimen, the lamella samples were cut out by a focused ion beam (FIB) using a Zeiss Auriga Crossbeam SEM-FIB according to the procedure described in [8]. Lamellae were cut from areas close to the surface of the HPT sample. The structure was also examined by X-ray diffraction (XRD) under Cu radiation employing a Rigaku Ultima IV device. The density measurements were performed in accordance with the precise technique of measuring the bulk density of small solid objects using laser confocal microscopy described recently in [11].

## 3. Results and discussion

According to the XRD and TEM studies, the initial MS Ti<sub>50</sub>Ni<sub>25</sub>Cu<sub>25</sub> alloys and Zr<sub>62</sub> BMG have a predominantly amorphous structure. TEM studies of the lamellae revealed a large number of shear bands in HPT-processed states (figure 1). The primary shear bands have an average thickness of 5-10 nm. The shear bands are distorted and assembled in a group or bundles. The average distance between the shear bands in a group ranges from 20 to 50 nm. In the HPT-processed Zr<sub>62</sub> BMG the groups of shear bands (zones of structural transformation with a banded contrast) have a total width of 200 nm and more (figure 1a). In the HPT-processed MS Ti<sub>50</sub>Ni<sub>25</sub>Cu<sub>25</sub> the groups of shear bands have a slightly smaller total width – up to 100 nm (figure 1b).

Nanocrystals were observed directly in shear bands in MS TiNiCu subjected to HPT (crystalline reflections in a microdiffraction pattern taken from the shear bands in figure 1b). These nanocrystals were formed as the result of strain-induced nanocrystallization, which was previously found in this amorphous alloy [2, 9]. There are areas with a cluster-type amorphous structure around the bundles of shear bands. The average size of clusters is 20-30 nm. According to the SAED pattern (figure 1b), the clusters have an amorphous structure. Probably, the clusters and their boundaries have different contents of free volume. However, the nature of the cluster-type amorphous structure in the HPT-processed MS Ti<sub>50</sub>Ni<sub>25</sub>Cu<sub>25</sub> has not been revealed yet.

The formation of a cluster-type amorphous structure after HPT was not detected in the Zr<sub>62</sub> BMG. Some fine crystalline reflections are also observed in the microdiffraction pattern taken from individual shear bands (figure 1a), which may also indicate the strain-induced nanocrystallization. However, nanocrystals were not observed on the most shear bands. Apparently, nanocrystallization in a shear band depends on the conditions of shear bands propagation. Thus, it can be concluded that the HPT-induced nanocrystallization in the Zr<sub>62</sub> BMG is less intensive than in the HPT-processed TiNiCu.

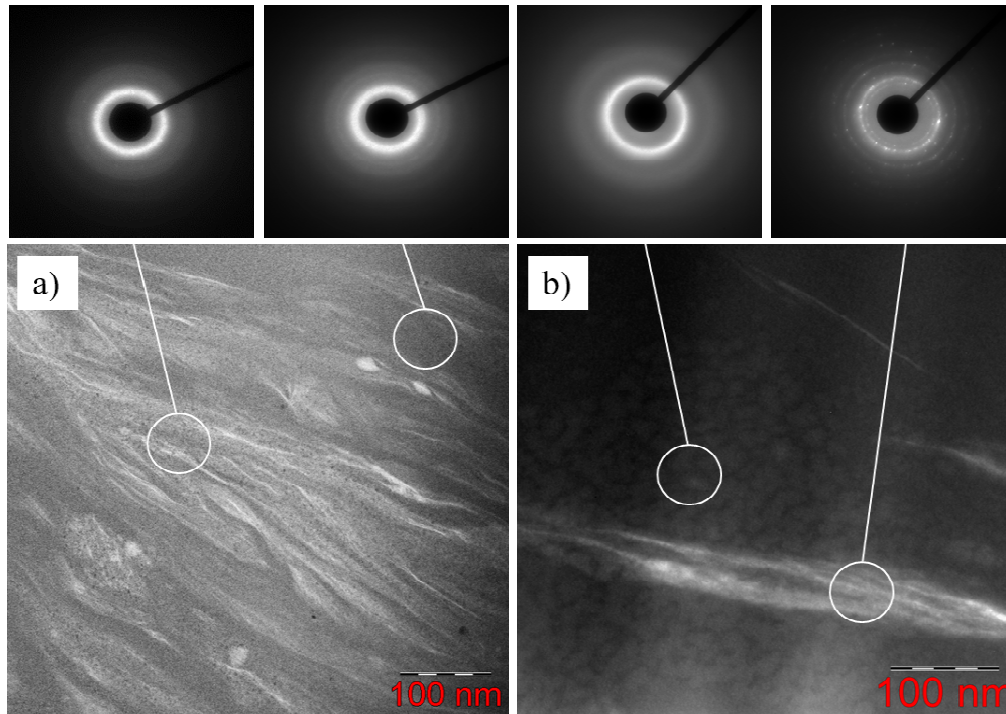


**Figure 1.** STEM BF image of a)  $Zr_{62}Cu_{22}Al_{10}Fe_5Dy_1$  BMG subjected to HPT, on the top – corresponding microdiffraction patterns from different regions of the sample. b) cluster-type amorphous structure and shear bands with nanocrystals of MS  $Ti_{50}Ni_{25}Cu_{25}$  subjected to HPT, on the top – corresponding microdiffraction patterns from different regions of the sample.

XRD shows the HPT-induced shift of the first diffraction halo to low angles for both alloys, which means an increase in the radius ( $R$ ) value of the first coordination sphere. This means an increase in the content of free volume ( $\Delta V$ ) [7]. The increment of free volume was calculated according to the procedure described in [7].  $\Delta V$  was increased approximately by 0.5 % in the HPT-processed  $Zr_{62}$  BMG compared to the initial state.  $\Delta V$  was increased approximately by 1.8 % in the HPT-processed MS  $Ti_{50}Ni_{25}Cu_{25}$  in comparison with the initial state. However, the analysis of changes in free volume, based on the shift of the first diffraction halo, may contain a considerable error for the MS  $Ti_{50}Ni_{25}Cu_{25}$  due to more intensive crystallization in this alloy. It should be noted that an increase in free volume leads to an increase in the ductility of amorphous alloys [12].

Density measurements performed according to the procedure [11] demonstrate that the initial  $Zr_{62}$  BMG has a density of  $\rho$  equal to  $6.98 \text{ kg/m}^3$ , which correlates with the data for bulk samples of this BMG obtained by hydrostatic weighing [13]. HPT processing leads to a decrease in the density values of the  $Zr_{62}$  BMG and the MS  $Ti_{50}Ni_{25}Cu_{25}$  ( $\Delta\rho$ ) approximately by 2%. The value of  $\Delta V=2 \%$  for the HPT-processed  $Zr_{62}$  BMG determined by the direct method, is much larger than  $\Delta V$  determined by XRD (0.5%). This is probably due to the fact that the HPT processing leads to the formation of nano-sized pores or cracks in the HPT-processed sample. Previously, nano-sized pores and nano-voids in the SPD-processed alloy were discovered in [14]. It should be noted that the increase in  $\Delta V = 0.5\%$  obtained by XRD in this work is close to  $\Delta V$  observed in other works on the HPT processing of BMGs [15].

#### 4. Conclusions

The direct density measurements and analysis of first diffraction halo shift demonstrate an increase in the free volume content in both amorphous MS  $\text{Ti}_{50}\text{Ni}_{25}\text{Cu}_{25}$  and  $\text{Zr}_{62}$  BMG. The formation of high density of shear bands in amorphous MS  $\text{Ti}_{50}\text{Ni}_{25}\text{Cu}_{25}$  and  $\text{Zr}_{62}$  BMG was detected on lamella samples using TEM. However, the structural transformations of these two amorphous alloys occur in different ways. HPT leads to the formation of groups of shear bands (zones of structural transformation with a banded contrast) with total width of 200 nm and more in  $\text{Zr}_{62}$  BMG, whereas groups of shear bands have a slightly smaller width – up to 100 nm in MS  $\text{Ti}_{50}\text{Ni}_{25}\text{Cu}_{25}$ . HPT-induced nanocrystallization in shear bands and the formation of a cluster-type amorphous structure were observed in MS  $\text{Ti}_{50}\text{Ni}_{25}\text{Cu}_{25}$ . The formation of nanoclusters was not observed in  $\text{Zr}_{62}$  BMG after HPT processing and strain-induced nanocrystallization is less prominent in this alloy. Additional studies are required for a deep understanding of the strain-induced structural transformations in amorphous alloys.

#### Acknowledgments

The authors acknowledge Saint-Petersburg State University for a research grant 6.65.43.2017. The work was partially supported by Deutsche Forschungsgemeinschaft (project number HA 1344/32-1. The scientific investigations were performed at the Interdisciplinary Resource Centre for Nanotechnology of the Research Park of St. Petersburg State University and center for collective use "Nanotech", Ufa State Aviation Technical University.

#### References

- [1] Meng F, Tsuchiya K, Seiichiro I and Yokoyama Y 2012 *Appl. Phys. Lett.* **101** 121914
- [2] Valiev R Z, Gunderov D V, Zhilyaev A P, Popov A G and Pushin V G 2004 *J. Metast. Nanocryst. Mater.* **22** 21
- [3] Wang X D, Cao Q P, Jiang J Z, Franz H, Schroers J, Valiev R Z, Ivanisenko Y, Gleiter H and Fecht H-J 2011 *Scripta Mater.* **64** 81
- [4] Gunderov D, Slesarenko V, Lukyanov A, Churakova A, Boltynjuk E, Pushin V, Ubyivovk E, Shelyakov A and Valiev R 2015 *Adv. Eng. Mater.* **17** 1728
- [5] Gunderov D V, Boltynjuk E V, Ubyivovk E V, Lukyanov A V, Churakova A A, Kilmametov A R, Zamula Y S and Valiev R Z 2018 *J. Alloys Comp.* **749** 612
- [6] Boltynjuk E V et al 2018 *J. Alloys Comp.* **747** 595
- [7] Shao H, Xu Y, Shi B, Yu C, Hahn H, Gleiter H and Li J 2013 *J. Alloys Comp.* **548** 77
- [8] Chen Y M, Ohkubo T, Mukai T and Hono K 2009 *J. Mater. Res.* **24** 1
- [9] Glezer A M, Sundeev R V and Shalimova A V 2011 *Dokl. Phys.* **56** 476
- [10] Abrosimova G and Aronin A 2018 *J. Alloys Comp.* **747** 26
- [11] Kilmametov A, Gröger R, Hahn H, Schimmel T and Walheim S 2017 *Adv. Mater. Technol.* **2** 1600115
- [12] Murali P and Ramamurty U 2005 *Acta Mater.* **53** 1467
- [13] Churyumov A Y, Bazlov A I, Zadorozhnyy V Y, Solonin A N, Caron A and Louzguine-Luzgin D V 2012 *Mater. Sci. Eng. A* **550** 358
- [14] Ribbe J, Schmitz G, Gunderov D, Estrin Y, Amouyal Y, Wilde G and Divinski S V 2013 *Acta Mater.* **61** 5477
- [15] Edalati K, Yokoyama Y and Horita Z 2010 *Mater. Trans.* **51** 23